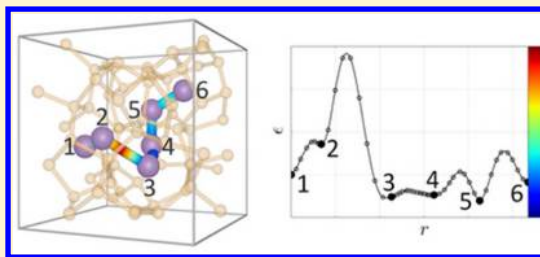# Diffusion of Lithium in Bulk Amorphous Silicon: A Theoretical Study

Georgios A. Tritsaris,[†] Kejie Zhao,[†] Onyekwelu U. Okeke,[‡] and Efthimios Kaxiras*[,†,‡]

[†]School of Engineering and Applied Sciences and [‡]Department of Physics, Harvard University, Cambridge, Massachusetts 02138, United States

**S** *Supporting Information*

**ABSTRACT:** The rate performance of lithium-ion secondary batteries depends critically on the kinetic transport of Li within the anode material. Here we use first-principles theoretical calculations to study the diffusion of Li in the low-concentration limit, using model electrodes of crystalline and four-fold coordinated bulk amorphous silicon. We identify Li diffusion pathways that have relatively low energy barriers (<0.50 eV) in amorphous silicon and discuss how diffusion at short (~2.5 Å), intermediate (~10 Å), and long (>1 nm) distances depends on the atomic-scale features of the silicon host. We find that both the energy barriers for diffusion and the topology of the atomic structure control the diffusion. We estimate the diffusion rate in amorphous Si anode to be comparable to the rate in crystalline Si anodes. These findings shed light on the wide range of reported experimental results for Li diffusion in Si anodes.

## INTRODUCTION

Li-ion secondary batteries are the subject of intense current interest as an energy storage technology of high energy density, suitable for portable and grid applications.[1−3] For instance, Si-based anodes have a high theoretical specific charge capacity of 4200 mAh g$^{-1}$, compared with 372 mAh g$^{-1}$ for graphite,[3−5] the conventional anode material in existing designs. In addition, Si is an abundant and environmentally friendly material. However, the commercialization of Si-based Li-ion batteries is at present severely constrained by the capacity loss caused by mechanical failure and chemical degradation of the Si anodes during battery operation.[6−8] Approaches for improving the rate performance of the Si anode include tailoring its geometry,[9,10] doping of the anode material,[11] and using amorphous Si (a-Si).[12−14]

The kinetics of Li diffusion is an issue of central importance to the mechanical failure of Si electrodes because it significantly affects the stress state during a lithiation cycle, and Li diffusivity is a key parameter in determining how fast a battery can be cycled.[15] A discrepancy exists in experimental reports of the diffusivity of Li in a-Si, with reported diffusivites spanning four orders of magnitude, between $10^{-14}$ and $10^{-10}$ cm$^2$ s$^{-1}$ with $10^{-12}$ cm$^2$ s$^{-1}$ a typical value.[16−19]

Density functional theory (DFT)-based methods can provide an atomic-level description of diffusion mechanisms in solids, which is a prerequisite for better understanding the process of lithiation and the kinetics of diffusion.[7,8,20−25] Here we report DFT calculations of the diffusion of Li in Si electrodes using atomic-scale models of the crystalline and amorphous environment, and we demonstrate how the structural features of the Si host can affect macroscopic properties of Li-ion batteries such as charge/discharge rates. We calculate energy barriers for the diffusion of Li atoms in crystalline silicon (c-Si) and in four-fold coordinated a-Si. We show that within our structural model for

a-Si there exist several pathways of relatively low energy barriers (<0.5 eV) for the diffusion of Li as well as a variety of other pathways with barriers as high as 2.4 eV. These barriers should be contrasted with the diffusion barrier in c-Si, calculated to be 0.55 eV and corresponding to a unique pathway in the crystalline lattice. We establish that not all of the diffusion pathways participate equally in mediating the flow of Li atoms in the material, even if all energy barriers were assumed to be equal. This indicates that the local atomic-scale structure of a-Si affects long-range diffusion not only through the energy barrier for the hoping of Li between low-energy sites but also through the connectivity and topology of the atomic network.

## METHODOLOGY

We used an amorphous bulk structure of 64 Si atoms with no coordination defects to model the a-Si battery anode. The structure is represented by a continuous random network model,[26] which, although it corresponds to an idealized case,[27] is suitable for studying a tractable number of diffusion pathways for Li. (See also the Supporting Information.) We calculated the diffusion barrier in c-Si using a diamond cubic supercell of 64 atoms, which is a 2 × 2 × 2 multiple of the conventional cubic cell that contains eight atoms. We performed total energy calculations with the SIESTA package[28] via the ASE interface.[29] A double-ζ plus polarization basis set was used to represent the Kohn–Sham orbitals. For the description of exchange and correlation, the PBE functional[30] was chosen.

To obtain diffusion pathways and the corresponding energy barriers, we employed standard nudged elastic band (NEB) calculations.[31] For each pair of configurations with Li in
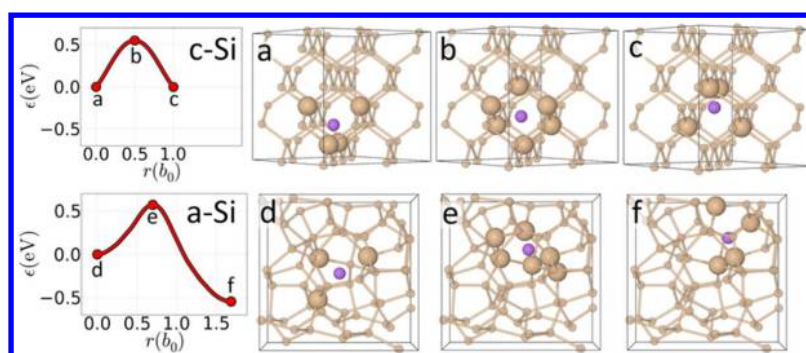
**Figure 1.** Diffusion of lithium atoms in bulk crystalline silicon (c-Si) and amorphous silicon (a-Si). The variation of the energy (red solid line) along the diffusion pathway is plotted against the diffusion length, $r$, given in units of the bond length, $b_0$, in c-Si ($b_0$ = 2.37 Å). Configurations (a) and (c) show the lithium atom (violet) at equilibrium sites and configuration (b) shows the lithium atom at the transition state between (a) and (c) in c-Si. The corresponding configurations in a-Si are labeled (d) and (f) for the equilibrium sites and (e) for the transition state. The silicon atoms that are nearest neighbors of lithium in each configuration are shown enlarged for contrast.

neighboring equilibrium sites, we sampled the corresponding pathway for diffusion with a NEB path consisting of eight intermediate configurations. The NEB path was first constructed by linear interpolation of the atomic coordinates. Then, the path was relaxed until the force on each atom was smaller than 0.05 eV/Å. Atoms more than 6 Å away from Li in all configurations were fixed to prevent the structure from drifting, and the shape and volume of the unit cell were also fixed. A continuous diffusion path was obtained by polynomial interpolation between the optimized configurations. For the analysis of the network of equilibrium sites, we used the NetworkX Python language package.[32]

## ■ RESULTS AND DISCUSSION

In this work, we study the limiting case of the diffusion of a single Li atom in a region of a-Si. Cooperative motion of Li and Si atoms during lithiation will affect the diffusion process,[24] and Si self-diffusion is relevant at higher concentrations of Li.[21] At low concentrations, we do not expect any self-diffusion of Si, and none was found in our simulations. Moreover, different kinetics describe the diffusion of Li on surfaces of Si and in bulk Si.[20,24] Here we focus on bulk Si as an appropriate starting point for understanding the fundamentals of Li diffusion. We discuss first the diffusion of a Li atom in c-Si as a reference process.

The first step in studying the diffusion pathways of impurities in solids is to establish stable configurations for the impurity atoms that correspond to local minima in the total energy. For the case of isolated Li impurities in c-Si, a unique site for the Li atom exists at an interstitial site referred to as the tetrahedral ($T_d$) position because of its symmetry: this site lies at a distance of $b_0$ away from a Si atom in the direction opposite from one of its nearest neighbor Si atoms, where $b_0$ is the bond length in the ideal Si crystal ($b_0$ = 2.37 Å, as obtained by our calculations from energy minimization as a function of the crystalline lattice constant). The diffusion process consists of the Li atom moving from one interstitial $T_d$ position to a neighboring one that is a distance $b_0$ away. In doing so, the Li atom passes through the hexagonal (Hex) interstitial position. The energy barrier of the process is $\varepsilon_{a,c-Si}$ = 0.55 eV. In the $T_d$ site, the Li atom has four Si nearest neighbors, whereas at the Hex site it has six Si nearest neighbors. In Figure 1, we show the atomic structures corresponding to the initial (labeled "a"), the barrier (labeled "b"), and the final (labeled "c") configurations as well as the energy change along the path. Long-range diffusion of Li in c-Si

consists of a series of steps in which the impurity atoms move randomly between $T_d$ sites by thermal activation and is isotropic because of the cubic symmetry of the host lattice.

In the case of a-Si, the task of determining the equilibrium positions of Li impurities in the amorphous network involves more steps because the structure is not invariant on the atomic scale. By analogy to the c-Si case, we start by placing the Li atoms at $T_d$-like sites in a-Si, defined as sites at a distance $b_0$ away from the Si positions and in a direction opposite to the Si–Si bonds of a given Si atom. The unit cell of the model a-Si structure comprises 64 Si atoms, each with four nearest neighbors to which it is covalently bonded. Therefore, a maximum of 256, in principle, distinguishable, interstitial $T_d$-like sites exist in the model, all lying on the extension of Si–Si bonds. With a single Li atom at each of those interstitial sites, we performed structure optimization where the unit cell was relaxed with respect to the atomic coordinates and cell shape, and we found that many of the initial $T_d$-like sites were very close both structurally and energetically. We employed hierarchical clustering to group the relaxed configurations into clusters using the distance between two Li atoms as the metric, with a cutoff of 0.6 Å (that is, $b_0/4$). The cutoff distance was chosen from a range of values that gave the smallest variation in the number of clusters. Within each cluster, the energy range of configurations was found to be no larger than 0.04 eV, and the lowest-energy configuration was used to represent the cluster. As a result of this clustering procedure, we identified 32 $T_d$-like equilibrium sites that we consider to be the unique (inequivalent) equilibrium sites of Li in the a-Si network of our model. (See also the Supporting Information.) We then used the NEB method to calculate the energy barrier for Li atoms moving between nearest neighbor equilibrium sites. Two energy barriers, $\varepsilon_{a,i\rightarrow j}$ and $\varepsilon_{a,j\rightarrow i}$, were calculated for the two directions of diffusion $p_{i\rightarrow j}$ and $p_{j\rightarrow i}$ between a pair of equilibrium sites labeled "i" and "j". Moreover, we calculate the average energy barrier for a single hop to be 0.58 eV and the average displacement $1.23b_0$, both comparable to the case of c-Si. In Figure 1, we show an example of a diffusion pathway in a-Si, described by the initial (labeled "d"), the barrier (labeled "e"), and final (labeled "f") configurations. The corresponding energy barrier is 0.57 eV. We also calculated the coordination using a cutoff distance 10% larger than the length of the shortest Si–Li bond with Li at a $T_d$ site in c-Si. Interestingly, the initial and final configurations for this pathway as well as the barrier configuration are structurally quite similar

to those found in c-Si; namely, in the initial and final configurations, the Li atom has three and four Si nearest neighbors, respectively, whereas in the barrier configuration, it has six Si nearest neighbors. In the entire a-Si model, the average number of Si neighbors of Li is 3.62 at the equilibrium sites and 5.54 at the transition state sites.

An important consideration for diffusion in a-Si is the long-range pathways and barrier(s) that the Li atoms encounter. Specifically, in contrast with c-Si, where each interstitial $T_d$ site for Li is always surrounded by other equivalent sites to which the Li can hop, this situation is not guaranteed to be valid in the a-Si network. The distribution of the low-energy $T_d$-like sites and the barriers between them is not necessarily uniform and continuous. To clarify these issues, we identified pathways for the diffusion of atomic Li in a-Si that consist of several hops between the equilibrium sites in sequences that lead to longer range displacement of the Li atoms. Figure 2 shows an example
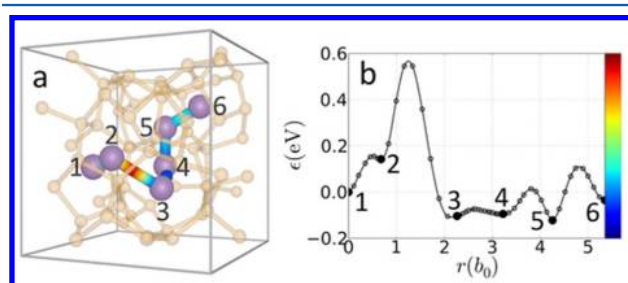


**Figure 2.** (a) Example of a pathway for the diffusion of a lithium atom (violet) in bulk amorphous silicon. The numbers label the equilibrium sites between which lithium hops. The path between the sites is colored with respect to the energy at each point. (b) Variation of the energy along the diffusion pathway: open circles mark nudged elastic band intermediate images between two equilibrium sites (black circles). The highest energy barrier is 0.43 eV between sites 2 and 3. The diffusion length $r$ is given in units of the bond length $b_0$ in bulk crystalline silicon ($b_0 = 2.37$ Å).

of a pathway with energy barrier lower than $\varepsilon_{a,c\text{-}Si} = 0.55$ eV and diffusion length comparable to the size of the unit cell. (The average side length of the unit cell is 11.3 Å.) In this example, the overall motion of the Li atom comprises five hops between the equilibrium sites labeled 1−2−3−4−5−6. The energy of the highest barrier is 0.43 eV (between positions 2 and 3, left to right). The total diffusion length, defined as the sum of distances traveled in each individual hop between equilibrium sites, is more than $5b_0 \simeq 12$ Å. The total displacement of Li, defined as the distance between initial and final equilibrium positions after five hops, is 7.57 Å.

To provide a more comprehensive picture of the diffusion process that takes into account both the barriers for longer range displacements and the topology of the moves that can lead to such displacements, we sampled diffusion pathways that cross up to six equilibrium sites. (The size of the model a-Si structure does not allow the study of more extended pathways.) Statistics of this analysis are summarized in Figure 3. Overall, the range of barriers is quite large from a minimum of 0.1 eV to a maximum of 2.4 eV. Most pathways have energy barriers higher than the barrier for diffusion in c-Si (0.55 eV), but a non-negligible number of pathways have smaller energy barriers. The average displacement of Li is calculated to be ~8.5 Å. There are relatively few pathways with an energy barrier around 1.5 eV, which we attribute to the features of the particular structural model of a-Si. Our findings suggest that
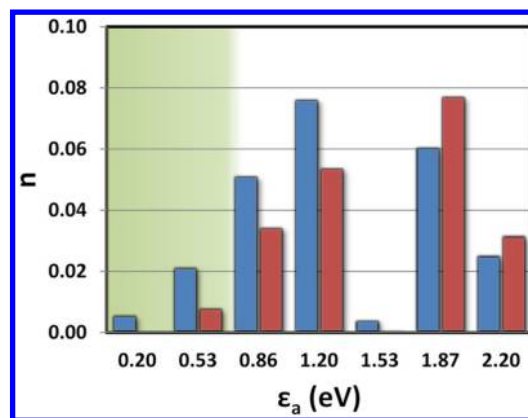


**Figure 3.** Distribution $n$ of pathways for the diffusion of atomic lithium in bulk amorphous silicon, with respect to the energy barrier $\varepsilon_a$. Blue columns correspond to displacement of lithium in the range 4.50 to 6.71 Å, and red columns correspond to displacement in the range 8.96−11.19 Å. Each column describes a range of energy barriers of $[-0.17,+0.17]$ eV. The number of pathways is normalized to the total number of diffusion pathways sampled (displacements up to ~10 Å).

studies of deformed lattices of c-Si[33,34] may not be sufficient in describing diffusion of Li in a-Si, unless the model allows for a distribution of energy barriers, or equivalently, for non-equivalent equilibrium sites for Li with respect to the local atomic environment.

To quantify these effects, we show in Figure 4 the network of the equilibrium sites and their connectivity for Li diffusion in
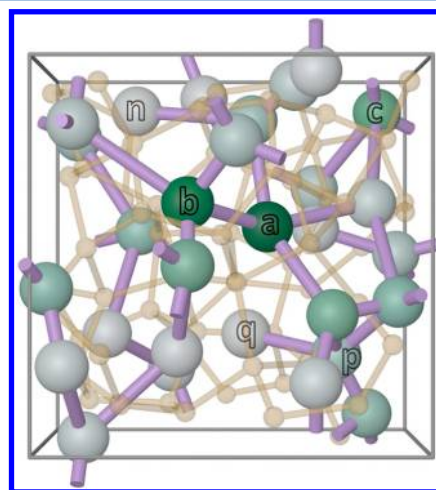


**Figure 4.** Equilibrium sites (opaque balls) and diffusion pathways (violet sticks) for lithium atoms in bulk amorphous silicon. At least one diffusion pathway exists between every two equilibrium sites. The sites are colored with respect to their relative significance (centrality) in mediating the flow of lithium (gray for low, dark green for high centrality), irrespective of the energy barriers for individual hops between sites.

the a-Si model structure. The average number of neighboring hoping sites, that is, the number of sites to which a Li atom can hop starting from any given equilibrium site, is 2.87. Not all of the equilibrium sites and therefore single diffusion hops participate equally in mediating the flow of Li, even if all energy barriers for diffusion were assumed to have the same value. To capture this, we define the concept of "centrality" of a site in the diffusion process. The centrality $c_i$ of a site labeled "i" is given by the expression $c_i = \Sigma \sigma_{j\to k}(i)/\sigma_{j\to k}$, where $\sigma_{j\to k}(i)$ is

the number of shortest pathways (determined by the number of nearest-neighbor hops) between sites labeled "j" and "k" that pass through site "i", and $\sigma_{j \to k}$ is the total number of shortest pathways between sites "j" and "k". The sum is taken over all sites, for j ≠ k, j ≠ i, and k ≠ i. We find that the sites with the highest $c_i$ are the neighboring sites labeled "a" and "b" in Figure 4, with $c_a = 1$ and $c_b = 0.93$, followed by site labeled "c" with $c_c = 0.65$ (normalized values are reported). Because of the relatively high centrality of the sites "a" and "b", and the high energy barriers between them ($\varepsilon_{a,1 \to 2} = 2.01$ eV, $\varepsilon_{a,2 \to 1} = 2.02$ eV), pathways such as $p_{a \to b}$ and $p_{b \to a}$ could act as a bottleneck for the diffusion of Li. Moreover, although at least one pathway exists between every two equilibrium sites (Figure 4), some sites, like the sites labeled "n" and "q", are accessible to the Li atom from only one neighboring site, which leads to $c_n = 0$ and $c_q = 0$. In addition, we find $\varepsilon_{a,p \to q} = 0.12$ eV, but $\varepsilon_{a,q \to p} = 1.46$ eV, which implies that diffusion toward site "q" is kinetically favorable but not in the opposite direction. Therefore, equilibrium sites such as "q" could act as trapping sites for Li atoms.[35]

The network of the equilibrium sites reflects the topology of the a-Si. In this sense, Figure 4 reveals the percolation of the equilibrium sites for Li and can provide insight into the measurable diffusion constant for Li in a-Si. Specifically, Figure 4 illustrates how lithiation can be controlled not only by local structural features but also by the topology of the Si host at intermediate length scales.[13,34] Knowledge of the energetics of the diffusion of Li alone may not suffice to explain the discrepancy in measured diffusivities. On the basis of the results obtained from this analysis, we attempt to address the experimental situation in what concerns diffusion of Li in a-Si. The diffusion constant is given by $D = d^2 \nu e^{-\varepsilon_a/kT}$, where d is the elementary hop distance, $\nu$ is the hoping frequency, $\varepsilon_a$ is the activation energy barrier, $k$ is the Boltzmann constant, and $T$ is the absolute temperature. Using the displacement and energy barrier, we found previously for c-Si (d = 2.37 Å, $\varepsilon_{a,c\text{-Si}} = 0.55$ eV), at $T = 300$ K (room temperature) and a typical value for $\nu = 10^{13}$ s$^{-1}$, we find for diffusion of Li in bulk c-Si: $D_{c\text{-Si}} = 3.6 \times 10^{-12}$ cm$^2$ s$^{-1}$, which is in the middle of the range of values ($10^{-14}$ and $10^{-10}$ cm$^2$ s$^{-1}$) that have been reported for the diffusivity of Li in a-Si.[16−18] The preceding analysis has shown that most of the pathways for Li diffusion at intermediate distances (∼10 Å) in a-Si are characterized by energy barriers that are higher than the barrier for diffusion in c-Si (see Figure 3), which suggests that the diffusivity of Li in a-Si should be smaller than that in c-Si. For example, assuming $\nu$ in a-Si to be comparable to that for c-Si, for $d = b_0$ and an average $\varepsilon_a = 0.70$ eV (that is, a barrier ∼20% higher than $\varepsilon_{a,c\text{-Si}}$), $D_{a\text{-Si}}$ is calculated to be on the order of $10^{-14}$ cm$^2$ s$^{-1}$. Still, because of the exponential dependence of the diffusivity on the energy barrier $\varepsilon_a$, there will be a significant contribution to the Li flow and thus to the charge/discharge rates, from diffusion pathways with low energy barriers. For example, for the pathway shown in Figure 2 ($d = 7.57$ Å/5 and $\varepsilon_a = 0.43$ eV), we calculate $D_{a\text{-Si}} = 1.04 \times 10^{-10}$ cm$^2$ s$^{-1}$, a relatively high diffusivity compared with c-Si. Pathways with low barriers constitute only a small percentage of the total number of available pathways (see Figure 3), which will reduce the overall rate from such low-barrier pathways. These arguments indicate that the lithiation rate measured in experiment will depend on both the energy barriers for diffusion and the topology of the atomic structure. It is likely that the evolution of the actual structure of a-Si with

each charge/discharge cycle produces changes in the local environment that can significantly affect the diffusivity.

To illustrate the relative importance of the low- and high-barrier pathways on extended length scales (>1 nm) and the interplay between energetics and topology in relation to experiment, we constructed a simplified model consisting of random networks of up to 200 equilibrium sites for Li (that is, six times more sites than the sites in the model a-Si structure used in the first-principles calculations). We ensured that there is at least one pathway that connects every two equilibrium sites and that the average number of Li nearest neighbors for each site is equal to or less than four. (The average number of neighbors in the model a-Si structure is 2.87.) We assigned a weight of $e^{-\varepsilon_a/kT}$ to each pathway between neighboring sites, with $\varepsilon_a$ chosen from a normal distribution centered at 0.55 eV. The centrality of each single-hop pathway was calculated by analogy to the case of the equilibrium sites previously discussed. Pathways with high centrality are expected to control a large part of the flow of Li acting as diffusion bottlenecks. We used the 5−25% pathways of higher centrality (we chose the exact percentage randomly) to calculate an effective value for the diffusivity of Li in the entire amorphous network. The entire process was repeated until the average of the diffusivities obtained was converged to within one order of magnitude. Through this procedure, we estimate the rate for long-range diffusion of Li in a-Si to be on the order of $10^{-12}$ cm$^2$ s$^{-1}$, which is comparable to the rate for diffusion in c-Si and in excellent agreement with experiments.[16,18] However, we stress that the considerations discussed above apply only to situations where Li impurities are isolated in a matrix of a-Si, which is relevant to low Li concentration (our model with one Li atom in a cell of 64 Si atoms translates into 1.5% Li content in a-Si). The situation at higher Li concentrations could be very different, with cooperative motion of the Li and Si atoms playing a large role in diffusion. In addition, measured diffusivity can vary in different stages of the charge/discharge cycle, even for a single cell.

## ■ CONCLUSIONS

We used first-principles total-energy calculations based on DFT to study the mechanisms of lithium diffusion in model electrodes of crystalline and four-fold coordinated amorphous silicon. We investigated pathways for the diffusion of atomic lithium in the material at short (∼2.5 Å), intermediate (∼10 Å), and extended (>1 nm) length scales. The energy barrier for diffusion between tetrahedral interstitial sites in crystalline silicon is 0.55 eV. In amorphous silicon, we find a distribution of energy barriers for elementary hops of Li atoms between equilibrium sites ranging from a low of 0.1 eV to a high of 2.4 eV. We identified pathways for the diffusion of lithium with relatively low energy barriers that consist of several elementary hops and lead to transport of lithium across distances that span the size of the amorphous model cell. The energy barriers for the diffusion are only one of the factors that control the diffusion process: not all of the diffusion pathways participate equally in mediating the flow of lithium in the material, even if all energy barriers were assumed to have the same value. In a simple extended model with the same distribution of equilibrium sites as in our atomic model for the amorphous Si structure, we find that the rate of long-range lithium diffusion is comparable to that in crystalline silicon (∼$10^{-12}$ cm$^2$ s$^{-1}$).

22215

dx.doi.org/10.1021/jp307221q | *J. Phys. Chem. C* 2012, 116, 22212−22216

## ASSOCIATED CONTENT

**S** Supporting Information

Structural model of amorphous silicon and positions of equilibrium sites for atomic lithium. This material is available free of charge via the Internet at http://pubs.acs.org.

## AUTHOR INFORMATION

**Corresponding Author**

*E-mail: kaxiras@physics.harvard.edu.

**Notes**

The authors declare no competing financial interest.

## ACKNOWLEDGMENTS

## REFERENCES

(1) Arico, A. S.; Bruce, P.; Scrosati, B.; Tarascon, J.-M.; van Schalkwijk, W. *Nat. Mater.* **2005**, *4*, 366−377.

(2) Dunn, B.; Kamath, H.; Tarascon, J.-M. *Science* **2011**, *334*, 928−935.

(3) Jeong, G.; Kim, Y.-U.; Kim, H.; Kim, Y.-J.; Sohn, H.-J. *Energy Environ. Sci.* **2011**, *4*, 1986−2002.

(4) Kasavajjula, U.; Wang, C.; Appleby, A. J. *J. Power Sources* **2007**, *163*, 1003−1039.

(5) Limthongkul, P.; Jang, Y.-I.; Dudney, N. J.; Chiang, Y.-M. *Acta Mater.* **2003**, *51*, 1103−1113.

(6) Wu, H.; Chan, G.; Choi, J. W.; Ryu, I.; Yao, Y.; McDowell, M. T.; Lee, S. W.; Jackson, A.; Yang, Y.; Hu, L.; et al. *Nat. Nanotechnol.* **2012**, *7*, 310−315.

(7) Zhao, K.; Wang, W. L.; Gregoire, J.; Pharr, M.; Suo, Z.; Vlassak, J. J.; Kaxiras, E. *Nano Lett.* **2011**, *11*, 2962−2967.

(8) Zhao, K.; Pharr, M.; Cai, S.; Vlassak, J. J.; Suo, Z. *J. Am. Ceram. Soc.* **2011**, *94*, s226−s235.

(9) Park, M.-H.; Kim, M. G.; Joo, J.; Kim, K.; Kim, J.; Ahn, S.; Cui, Y.; Cho, J. *Nano Lett.* **2009**, *9*, 3844−3847.

(10) Zhang, Q.; Zhang, W.; Wan, W.; Cui, Y.; Wang, E. *Nano Lett.* **2010**, *10*, 3243−3249.

(11) Long, B. R.; Chan, M. K. Y.; Greeley, J. P.; Gewirth, A. A. *J. Phys. Chem. C* **2011**, *115*, 18916−18921.

(12) Bourderau, S.; Brousse, T.; Schleich, D. M. *J. Power Sources* **1999**, *81−82*, 233−236.

(13) Chevrier, V. L.; Dahn, J. R. *J. Electrochem. Soc.* **2009**, *156*, A454.

(14) Jung, H.; Park, M.; Yoon, Y.-G.; Kim, G.-B.; Joo, S.-K. *J. Power Sources* **2003**, *115*, 346−351.

(15) Zhao, K.; Pharr, M.; Vlassak, J. J.; Suo, Z. *J. Appl. Phys.* **2011**, *109*, 016110.

(16) Ding, N.; Xu, J.; Yao, Y. X.; Wegner, G.; Fang, X.; Chen, C. H.; Lieberwirth, I. *Solid State Ionics* **2009**, *180*, 222−225.

(17) Ruffo, R.; Hong, S. S.; Chan, C. K.; Huggins, R. A.; Cui, Y. *J. Phys. Chem. C* **2009**, *113*, 11390−11398.

(18) Xie, J.; Imanishi, N.; Zhang, T.; Hirano, A.; Takeda, Y.; Yamamoto, O. *Mater. Chem. Phys.* **2010**, *120*, 421−425.

(19) Yoshimura, K.; Suzuki, J.; Sekine, K.; Takamura, T. *J. Power Sources* **2007**, *174*, 653−657.

(20) Chan, T.-L.; Chelikowsky, J. R. *Nano Lett.* **2010**, *10*, 821−825.

(21) Johari, P.; Qi, Y.; Shenoy, V. B. *Nano Lett.* **2011**, *11*, 5494−5500.

(22) Kim, H.; Chou, C.-Y.; Ekerdt, J. G.; Hwang, G. S. *J. Phys. Chem. C* **2011**, *115*, 2514−2521.

(23) Shenoy, V. B.; Johari, P.; Qi, Y. *J. Power Sources* **2010**, *195*, 6825−6830.

(24) Wan, W.; Zhang, Q.; Cui, Y.; Wang, E. *J. Phys.: Condens. Matter* **2010**, *22*, 415501.

(25) Zhao, K.; Tritsaris, G. A.; Pharr, M.; Wang, W. L.; Okeke, O.; Suo, Z.; Vlassak, J. J.; Kaxiras, E. *Nano Lett.* **2012**, *12*, 4397−4403.

(26) Mo, Y.; Bazant, M. Z.; Kaxiras, E. *Phys. Rev. B* **2004**, *70*, 205210.

(27) Treacy, M. M. J.; Borisenko, K. B. *Science* **2012**, *335*, 950−953.

(28) Soler, J. M.; Artacho, E.; Gale, J. D.; García, A.; Junquera, J.; Ordejón, P.; Sánchez-Portal, D. *J. Phys.: Condens. Matter* **2002**, *14*, 2745−2779.

(29) Bahn, S. R.; Jacobsen, K. W. *Comput. Sci. Eng.* **2002**, *4*, 56−66.

(30) Perdew, J. P.; Burke, K.; Wang, Y. *Phys. Rev. B* **1996**, *54*, 16533−16539.

(31) Henkelman, G.; Uberuaga, B. P.; Jónsson, H. *J. Chem. Phys.* **2000**, *113*, 9901.

(32) Hagberg, A. A.; Schult, D. A.; Swart, P. J. In *Proceedings of the 7th Python in Science Conference*; Varoquaux, G., Vaught, T., Millman, J., Eds.; Pasadena, CA, 2008; pp 11−15.

(33) Popov, Z.; Fedorov, A.; Kuzubov, A.; Kozhevnikova, T. *J. Struct. Chem.* **2011**, *52*, 861−869.

(34) Huang, S.; Zhu, T. *J. Power Sources* **2011**, *196*, 3664−3668.

(35) Dimov, N.; Kugino, S.; Yoshio, M. *Electrochim. Acta* **2003**, *48*, 1579−1587.